Numerical simulation and additive manufacturing technology in design of knee implant patterns

ALEKSANDAR RAJIC[a]*, ELEONORA DESNICA[b], SLOBODAN STOJADINOVIC[b], DORIAN NEDELCU[c]

[a]*Technical College of Applied Sciences in Zrenjanin, Zrenjanin, Republic of Serbia*
[b]*Technical Faculty "Mihajlo Pupin", Zrenjanin, University of Novi Sad, Republic of Serbia*
[c] *"Eftimie Murgu" University of Resita, Resita, Romania*

The paper presents the possibilities to apply Numerical Simulation and Additive Manufacturing (AM) technology in designing the prototypes of master patterns of knee implants for investment casting. The master pattern manufacturing by wax injection is the starting operation in the investment casting procedure. Errors caused by shrinkage, air traps and the lower quality of surface roughness may occur in the wax injection process. The software SolidWorks Plastics was used in this research in order to avoid these errors. The software analyzed the fill time, gate location, temperatures and pressures. The second part of the research presents the comparison of different AM processes (Selective Laser Sintering, 3D Printing and PolyJet) considering the characteristics of the material and the manufacturing time of the prototypes of knee implant patterns.

1. Introduction

The focus of the modern trends in development of investment casting procedure lies on development of very complex thin-walled moulds with high dimensional accuracy requirements and high strength and special properties. The starting phase in investment casting is the development of wax patterns and most experts in this area believe that the quality of the final casting depends on the wax model and may be only as good as the wax pattern. The key factors affecting the errors in wax injection are the non-equilibrium filling process and non-uniform cooling.

The interaction of wax rheological properties with injection parameters has been ignored by engineers in foundries and they have generally used the standard trial-and-error method and relied on their experience. This resulted in long manufacturing cycle, high costs, low-grade of the moulds and the wax patterns.

Numerical simulation has proved to be an efficient method in mould design and the design of the injection process parameters. One of the main problems that the application of this method meets is the lack of constitutive equations and the material properties used for the industrial wax. It is necessary to take into consideration all the thermophysical and rheological parameters of the wax injection process before starting any simulation work. The standard test methods used for investigation of polymeric materials should be adapted in order to obtain valid properties of the wax. Otherwise, it would be impossible to predict the wax flow behaviour.

The recent researches in numerical simulation of wax injection and the application of the Additive Manufacturing (AM) technologies in investment casting procedure will be considered in the following part of the paper.

Bonilla found that the injection parameters played an important role in the accuracy of the wax patterns. These parameters included: the injection flow rate, the injection cycle time, the injection temperature, the injection pressure, and the mould temperature [1].

Gebelin and Jolly fully characterized the rheology of wax with Carreau model and Second-Order model for the purpose of modelling its injection process for the investment casting process. Gebelin reported that it was possible to model accurately the filling of a mould during the wax injection process, in both liquid and paste state [2].

Sabau et al. used the computer models to determine wax pattern dimensions taking into account the thermophysical and rheological behaviour of the wax. Pattern dimensions were calculated using a 3D finite element model for coupled thermal and mechanical analysis developed within the commercial software Abaqus. The results of numerical simulation were compared with experimental measurements on test patterns [3].

Bo et al. used the measurement techniques developed for polymeric materials in behaviour simulation of industrial wax. Based on generalized non-Newtonian fluid with seven parameters of Cross-WLF viscosity model, the injection process of wax was simulated with a 3D model. The Moldflow software was used for simulation and the best gate location and the injection channel system were defined. The results obtained by the simulation using the "Fusion" model show a good predictability in wax shrinkage behaviour in the thin-walled parts [4].

Radu et al. experimentally confirmed the results obtained by the injection simulation in the Autodesk Moldflow software in order to obtain optimal process parameters including the gate location, number and positions of the vents. The technological characteristics of four types of the wax were analyzed in the experimental research as well as the volume of the air traps, the optimal manufacturing parameters and the dimensional accuracy of the produced parts. Based on the researches conducted by AM technology, a master model was made and in the later phase, a wax model with accurate dimensions was made following the procedure of vacuum casting [5].

One of the primary uses of Additive Manufacturing technology is to quickly produce prototypes for model validation and testing purposes. Presently, almost all commercialized AM techniques have been employed to produce casting patterns with varying success and many AM solutions in investment casting are being used by various industries and researchers. The use of AM in investment casting is found in three basic forms. Fig. 1 shows the three basic approaches used as rapid casting solutions in Rapid Investment Casting (RIC) [6], [7].
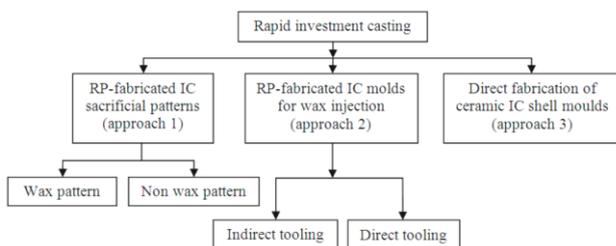

Fig. 1. Rapid investment casting approaches [7].

In their paper, Horacek et al. showed the manufacturing technology for making prototypes used in orthopaedic surgery using the technology of rapid development of prototypes and the investment casting procedure. A new approach was proposed in the paper which would enable the manufacturing of the total knee replacement individually adjustable. The authors showed that by using the CT scan it was possible to manufacture a custom knee implant, which would considerably minimize the invasiveness of surgical procedure and shorten the time for the implant manufacturing [8].

Maji et al. reported the possibility to use rapid investment casting technology to obtain craniofacial implants manufactured from bio-compatible materials. The research was conducted using the following process series: 3D CAD - Rapid Prototyping - Rapid Tooling – Investment casting. Aluminium craniofacial implants were manufactured and since aluminium is not a bio-compatible material, further researches will include application of bio-compatible materials [9].

Ramos et al. showed the development of technical procedure for hip prototype implant manufacturing. The authors reported that the vacuum casting technique combined with RTV (room temperature vulcanization) procedure was suitable for manufacturing of master patterns for investment casting of some prototypes. They

concluded that the tested technical procedure was acceptable for manufacturing of many cheap metal prototypes with excellent characteristics and functionality [10].

The study presented in this paper represents a part of the developed research in design, 3D numerical simulation analysis and development of knee implant master pattern. The purpose of this study was to analyze the fill time and the gate location for the wax model of knee implant. In researches involving numerical simulation of wax behaviour during injection which have been conducted so far, the Moldflow software was mainly used. However, the SolidWorks Plastics software, fully integrated in the SolidWorks simulation package, was used for this research. It enabled simulation of the injection process and changes based on the injection results.

In the second part of the study the preparation of the model and the parameters of the printing process were analyzed as well as the manufacturing of the master pattern of the femoral components of the total knee replacement using different AM processes: Selective Laser Sintering (SLS), 3D Printing (3DP) and PolyJet Printing (PJP). The prototypes manufactured in this study were intended for education of the students and for further researches.

2. Modelling of the knee implant pattern

In order to successfully conduct the numerical simulation of injection and to report the wax behaviour during injection, it was necessary to digitalize a real model and to convert it into a shape recognizable by the computer. A femoral component of the total knee joint endoprosthesis was chosen as the initial model in this study. Until a few years ago, it had been manufactured in the Foundry of investment castings Ada (Serbia) for orthopaedic purposes and the total knee replacement (TKR) surgery [11].

One of the most important aspects of TKR surgery is to design better knee implants in the operation. The knee joint consists of three bones: the femur, the tibia, and the patella as shown in Fig. 2 (a). The two major bones related to TKR surgery are the femur and the tibia. Similarly, a knee implant consists of the femoral, the tibial, and the patellar component as shown in Fig. 2 (b). The metal femoral component displaces the bottom of the femur and has a groove so the patellar component can glide up and down smoothly [12].
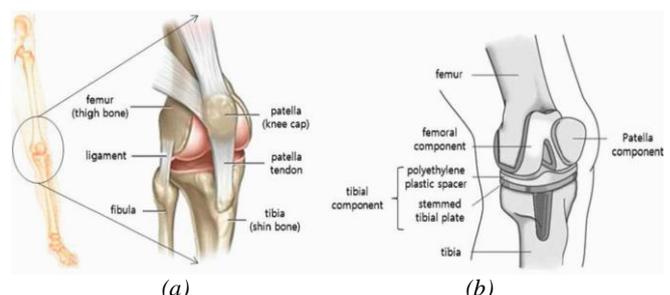

(a)   (b)
Fig. 2. Knee bones: (a) anatomy of the normal knee, (b) knee implants [12].

In the first phase of the research the selected sample of the knee implant was scanned by the optical 3D scanner OptiNum (Noomeo, France) and saved in ASCII format using Numisoft software.

The digitalization of the knee implant physical model involved the use of modern equipment with output databases suitable for converting into databases compatible with the SolidWorks software used for adjusting the scanned models.

Due to a small differences generated by the scanner while recognizing the geometry, the obtained scanned model shown in fig. 3 (a) was not an entirely true copy of the original, so the output databases were imported in the SolidWorks software package for modelling. Within this package the geometry was adjusted, completed and converted in STL format and prepared for exporting in the SolidWorks Plastics module. Fig. 3 (b) shows the CAD solid model obtained using the optical scanner Noomeo OptiNum.
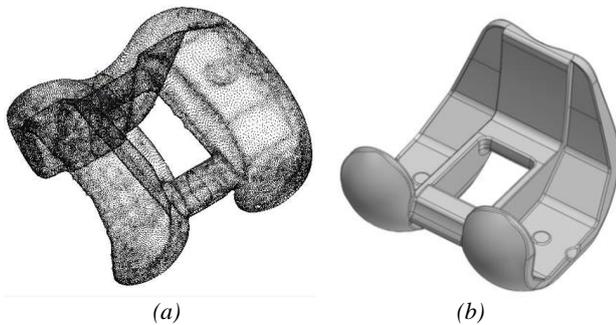

(a)   *(b)*
Fig. 3. Visual display of the model obtained using optical scanner: (a) point cloud (1729003 points), (b) SolidWorks solid model.

The developed model is parametric, i.e. lengths and radii are not of fixed but changeable values, so new models with different lengths and radii may be obtained simply by changing the initially given parameters. This provides an efficient way of obtaining new shapes of implants in short time intervals to analyze the most appropriate geometry for specific prosthesis requirements.

3. Wax pattern rheological properties and injection simulation

The wax used for the model developing was made from paraffin of high molecular weight with addition of the coal tar pitch. Linear shrinkage depend more on the method of work, pressure and the solidification time than on the wax temperature. Apart from the wax, plastics as mixtures of natural types of wax, synthetic wax and hydrocarbon resins in different proportions, are also used.

The complexity of the modelling wax composition is the main reason for the complexity of its rheological behaviour. All subsequential dimensional changes during the phases: development of the master pattern, shell formation, deparaffinization, shell drying and firing, metal

melting, mould solidification and cooling down, must be taken into consideration to form an optimal model for the wax injection cycle.

Predicting the wax behaviour during injection implies an analysis of a great number of thermophysical values, such as: heat capacity and conductivity of the wax, wax viscosity, heat transfer coefficient between the wax and the mould. During the process of investment casting, while still a liquid, wax behaves as a Newtonian fluid, while in a semi-liquid state it behaves as a non-Newtonian fluid.

Newtonian flow occurs at lower shear rates, but with increasing shear, the viscosity tends to fall away in what is termed shear-shinning behaviour. The polymer viscosity is a function of shear rate and temperature, as is shown in Fig. 4. In modelling the viscosity, a Cross-WLF type equation is used. This model contained seven unknown parameters: D1, D2, D3, A1, A2, τ^* and n.

The Cross-WFL viscosity model describes the temperature, shear rate and pressure dependency of the viscosity (η). The viscosity model is given by the following equations:

$$\eta = \frac{\eta_0}{1+\left(\frac{\eta_0 \dot{\gamma}}{\tau^*}\right)^{1-n}} \qquad (1)$$

In the equations η_0 represents zero shear viscosity, $\dot{\gamma}$ is the shear rate, τ^* is the critical stress level at the transition to shear thinning and n is the power law index in the high shear rate regime.

The zero shear viscosity is given by the equations:

$$\eta_0 = D_1 \exp\left[-\frac{A_1\left(T-T^*\right)}{A_2+\left(T-T^*\right)}\right] \qquad (2)$$

$$A_2 = A_3 + D_3 p \qquad (3)$$

In the equations T represents temperature, T^* is the glass transition temperature, p is the pressure. D_1, A_1, A_2 and D_3 are data- fitted coefficients.

The glass transition is given by equation:

$$T^* = D_2 + D_3 p \qquad (4)$$

In the equation D_2 is data-fitted coefficient.

SolidWorks Plastics, which is well known as plastic injection molding CAE software, could build a mathematic model based on Cross-WLF functional form. The wax Paracast FW 13070 is defined in the SolidWorks Plastics material database as a new material. Its basic parameters are also defined using the data obtained by the manufacturer Paramelt BV, the Netherlands.

Paracast FW 13070 is a filled pattern wax (27-29 %) composed by mixture of refined hydrocarbon waxes, polymers, resins and (if coloured) pigments. Fig. 4 shows the evolution of the viscosity as a function of the shear rate obtained from SolidWorks Plastics user-defined databank.
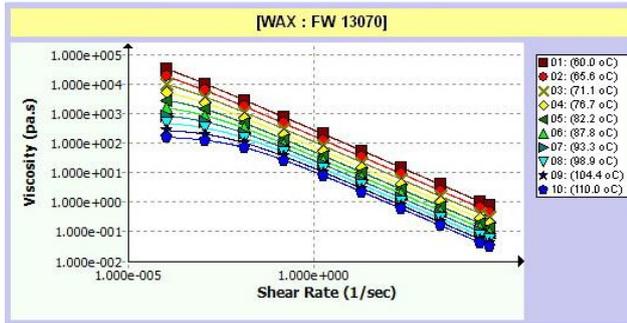
Fig. 4. Viscosity curve.

Table 1 shows the basic technical specifications of the wax Paracast FW 13070.

Table 1. Technical specifications of the wax.

Technical data	Specifications	Method
Colour	Green	Visual
Drop melting point [°C]	67-73	ASTM D 3954
Congealing point [°C]	63-69	ASTM D 938
Viscosity at 80°C [mPa.s]	300-500	ASTM D 3236
Viscosity at 90°C [mPa.s]	225-325	ASTM D 3236
Ash content [%]	Max 0.05	
Flame point [°C]	>190	

The Numerical simulation of the wax injection process was made according to the manufacturer's recommendations with parameters given in the Table 2.

Table 2. The recommended injection parameters.

Parameters	Values
Mould temperature [°C]	25
Melt temperature [°C]	69
Injection temperature [°C]	45
Injection rate [cm³/s]	10
Packing time [s]	9.17

A semi-automatic machine MPI55 for wax injection was defined in the simulation with a maximum injection pressure of 7 MPa, a maximum injection rate of 200 cm³/s and a maximum clamp force of 22.6 t.

The analysis of the wax material flow used in the injection process was done by SolidWorks Plastics and it goes through usual stages. The numerical simulation was carried out to check the technological workability of appropriate cavity filling. SolidWorks Plastics offers the options of controlled flow of injection through the volume (absolute control) or through the fill time (relative control). The absolute control option was chosen for the research so the simulation gave different fill times.

The results of SolidWorks Plastics simulation are presented in chapter 5.

4. Additive Manufacturing of knee implant master patterns

In this part of the research different AM models were produced which may be used as a starting point to obtain master patterns for the investment casting procedure. Different AM processes were analyzed and compared regarding consumption and characteristics of the applied materials, time and characteristics of the printing process.

The processes, systems and materials used for manufacturing of the AM model in the research were the following:
- Selective Laser Sintering (SLS), Formiga P100, PA2200;
- 3D Printing (3DP), Spectrum Z510, zp151;
- PolyJet 3D Printing (PJP), Objet 30, VeroBlack FullCure 870.

4.1. Selective Laser Sintering (SLS) technology

The knee implant models were manufactured on the Formiga P100 machine in the laboratory "3D Impuls" at the Faculty of Mechanical Engineering and Construction in Kraljevo, Serbia (http://www.3dimpuls.com/en). The development of the model on this machine was based on the technology of Selective Laser Sintering (SLS).

The SLS process was developed at the University of Texas in Austin (USA) while the company DTM (Austin, USA) was responsible for the commercialization process. Since 2001 the SLS has been owned by the company EOS GmbH (Electro Optical Systems, Germany).

Unlike the PolyJet process where the layers are formed by extruding the photopolymers and the support materials from the nozzles, in the SLS process a laser is used to sinter the particles of a material. Instead of the liquid photopolymer, in the SLS process various powdered materials are used.

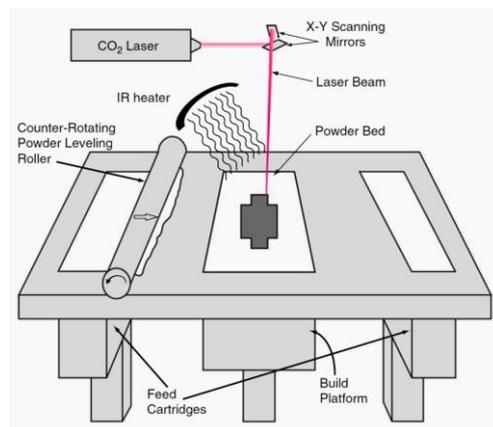The schematic representation of the SLS process is given in Fig. 5.

Fig. 5. Schematic representation of the SLS process [7].

Table 3 shows the basic technical parameters of Formiga P100 [14].

Table 3. Basic technical parameters of Formiga P100.

Printer dimensions [mm] (L x W x H)	1320 x 1067 x 2204
Printer weight [kg]	600
Working space [mm] (X x Y x Z)	200 x 250 x 330
Production space [mm] (X x Y x Z)	180 x 230 x 300
Layer thickness [mm]	0.06~0.12
Build material	PA 2200
Software	EOS RP-Tools

Formiga P100 (Fig. 6) machine is designed for working with plastic materials in direct manufacturing of small series and prototyping of functional spare parts.

Figure 6. Formiga P100 EOS SLS machine.

The rational positioning of the parts within the building area is based on uniform distribution of the melting areas during the manufacturing (Fig. 7). A part agglomeration in a certain area having the same Z positions could lead to a local temperature enhancement, influencing the stability of the job [15].
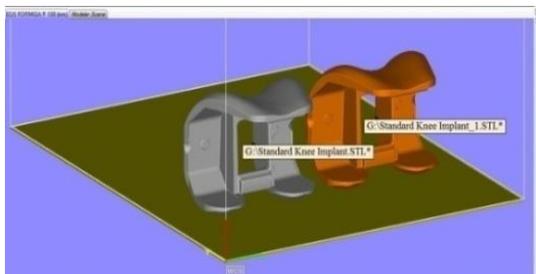

Fig. 7. SLS parts positioning on the building platform.

The preparation of the printing model was done in Magics, EOS RP-Tools and PSW. The Magics software was used to position the parts on the working platform with 5 mm distance between them to avoid the heat effect between the neighbouring parts. EOS RP-Tools was used to define the layer thickness of 0,1 mm, to slice the file at the layer thickness and to verify and correct the layers. In the PSW software, the material and the parameters of the process were assigned and the executable file was verified only to be exported into the machine. The process of printing the model was started automatically upon reaching the operating temperature of the chamber of 172 °C.

The laser power value during the sintering process depends on the type of the material and the thickness of the layer. By changing the CO_2 laser parameter, the quality of the surface roughness, dimensional accuracy and time of manufacturing can be changed as well. The density of the laser beam energy may improve the connections between the sintering particles and the mechanical properties of the part on the contour layers and the hatch layers as well. According to the previous studies the energy density depends on the power and speed of the laser beam and on the hatch distance and is calculated according to the following equation [16]:

$$E_A = P / (U \cdot SP) \qquad (5)$$

were E_A [J/mm^2] is energy density, P [W] is laser power, U [mm/s] is scan velocity and SP is the hatch spacing between parallel scan lines.

The laser power used in experiment was P = 25 [W], the scanning velocity was U = 2540 [mm/s] and the hatch spacing was SP = 0.26 [mm]. After 5 hours the machine and the parts had been cooled down, the parts were removed, cleaned and washed. Fig. 8 shows the printing process of the SLS knee implants.

Fig. 8. SLS printing process of the knee implants.

4.2. 3D Printing (3DP) technology

The knee implant models were manufactured on the Spectrum™Z510 machine owned by the company "3D Svet" from Belgrade (http://www.3dsvet.rs/site/). The developing of the models on this machine is based on 3D Printing (3DP) technology. Unlike the printing processes described earlier, 3DP prints a binder into a powder bed to manufacture a part. Hence, in 3DP, only a small portion of the part material is delivered through the print-head; most of the part material is composed of powder in the powder bed. Typically, binder droplets form spherical agglomerates of binder liquid and powder particles and provide bonding to the previously printed layer. Once a layer is printed, the powder bed is lowered and a new layer of powder is spread onto it, very similar to the recoating methods used in SLS processes, as presented earlier. This

process is repeated until the part or the array of parts, is completed. A schematic of the 3DP process is shown in Fig. 9.
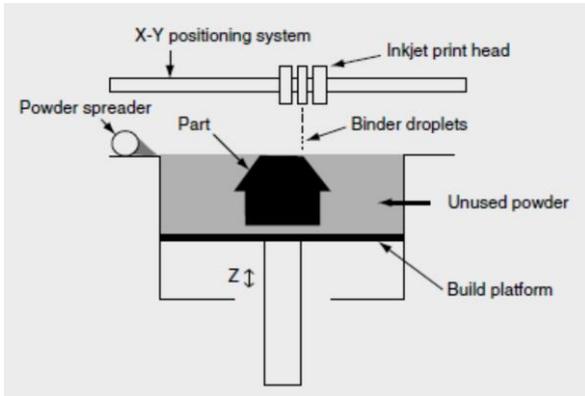

Fig. 9. Schematic of the 3D Printing process [7].

Table 4 shows the basic technical parameters of Spectrum Z510 [17].

Table 4. Basic technical parameters of Spectrum Z510.

Printer dimensions [mm] (Lx W x H)	1870 x 740 x 1450
Printer weight [kg]	340
Working space [mm] (X x Y x Z)	254 x 381 x 203
Layer thickness [mm]	0.089 - 0.102
Resolution [dpi]	600 x 540
Build material	zp151
Software	Z Print

After printing, the part is removed from the powder bed, depowdered and dried. The part can then be infiltrated with wax, epoxy, or other materials to increase strength and durability. Because the powder layers support the structures being printed, the printer creates parts without support structures and will print parts with complex geometries. Spectrum Z510 system (Fig. 10) used in this study excel as low cost fast prototyping machines.

Fig. 10. Spectrum Z510 system.

Z Print (Fig. 11) is software for preparing and optimizing the build area. The software will place the parts within the build box to maximize build speed. The smallest dimension of parts must be placed along the Z-axis (vertical). The parts will be strongest along Y-axis and X-axis and less strong along Z-axis. This is because the cross section are printed in continuous strips along the Y or the "fast" axis, bands across the X or the "slow" axis and laminated layers along the Z-axis.
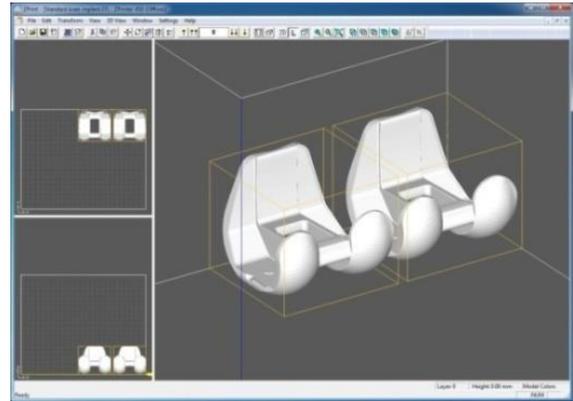

Fig. 11. The STL file of the knee implants loaded in Z Print software and placed on printer tray.

Fig. 12. shows the printing process of the knee implants by 3DP technology.

Fig. 12. Knee implants manufactured by 3DP technology.

4.3. PolyJet 3D Printing (PJP) technology

The knee implant models were manufactured on the Objet30 Stratasys machine in the "Centre for Numerical Simulation and Digital/Rapid Prototyping" at the Faculty of Engineering and Management, Resita, Romania (http://www.csnp.roedu.ro/index_eng.htm).

The development of the models on this machine is based on the PolyJet technology. The principle is very similar to 2D printing process of inkjet pointer and it is shown on Fig. 13.
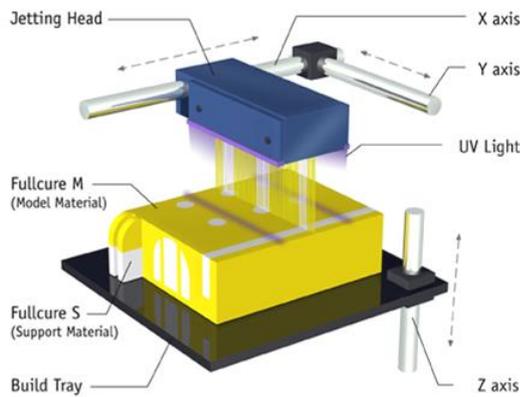
Fig. 13. Basic principle of PolyJet printing process [7].

The injected material is a polymer which after cooling forms the required layer or binder which bonds powder particles. The process consists only of UV bulbs and photopolymer materials. Objet 30 printer (Fig. 14) fully cure each layer of super fine UV photopolymer and support materials as eight jetting heads precisely deposit the product. Support material is easily separated from the part by either a water jet or hand and brush. No special baths or extra finishing treatments are needed [18], [19].

Fig. 14. Objet 30 3D Printer.

Table 5 shows the basic technical parameters of Objet 30 [20].

Table 5. Basic technical parameters of Objet 30.

Printer dimensions [mm] (Lx W x H)	825 x 620 x 590
Printer weight [kg]	93
Working space [mm] (X x Y x Z)	300 x 200 x150
Production space [mm] (X x Y x Z)	294 x 192 x 148.6
Layer thickness [mm]	0.028
Resolution [dpi]	600 x 600 x 900
Build material	Vero Black FullCure 870
Software	Objet Studio

Models that are saved in a CAD program as STL files may be inserted into the Objet Studio tray. Fig. 15 shows the STL files loaded in Objet Studio software. The orientation of models on the build tray affects how quickly and efficiently they will be produced by the 3D printer, where and how much support material is used, and whether or not model parts will have a gloss finish.
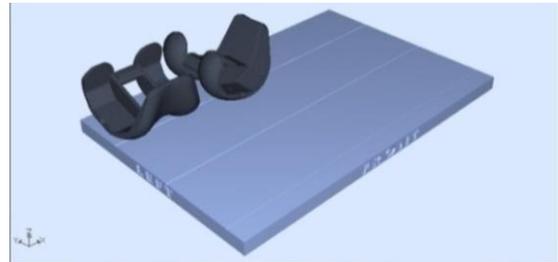

Fig. 15. The STL file of the 2 knee implants loaded in Objet Studio software and placed on printer tray.

To minimize the print time: the longest dimension of a model must be placed along the X-axis, the smallest dimension of a model must be placed along the Z-axis and the tallest model must be placed on the left of the tray.

When a tray is ready to be printed, it is sent to Job Manager, where it is placed in the print queue. When the job reaches the head of the queue, Job Manager pre-processes the tray file to create slices, and feeds them to the 3D printer.

For optimal efficiency the two knee implants were manufactured along with a number of other parts. Fig. 16 shows the printing process of the knee implants.

Fig. 16. Printing process of the knee implants by PJP technology.

5. Results and discussion

Two types of meshes were used in the SolidWorks Plastics simulation: Solid and Shell, while the analysis type was Flow/Pack/Warp.

The mesh model of Solid type used in the simulation had 12186 elements and 11927 points, while the mesh model of Shell type had 10623 elements and 50305 points

Three different gate locations were considered and shown in figures 17 (a), 17 (b) and 17 (c). In Version A shown in Fig. 17 (a) an automatic defining of the gate

location was assigned, while in versions B and C shown in Fig. 17 (b) and 17 (c) the gate locations were defined manually.

Table 6 shows the calculated fill times for different types of meshes and gate locations.

Table 6. Fill times of different gate locations

Mesh type	Fill time for gate location A [s]	Fill time for gate location B [s]	Fill time for gate location C [s]
Solid	5.6858	5.7749	5.6727
Shell	3.6812	3.6844	3.6807

In versions A and B some inhomogeneous cavity fillings may be noticed on thin central walls. These inhomogeneous filings resulted in the non-uniform shrinkage and the deformation of the wax model in the central area. In the C version the gate location was on the front side of the central bridge which is the thickest part of the model.

In version C the fill time was the shortest with a uniform cavity filling which indicated the lower percentage of deformation and a more accurate wax model. The version C shown in Fig. 17 (c) was adopted as an optimal solution with the gate location on the front side of the central bridge.
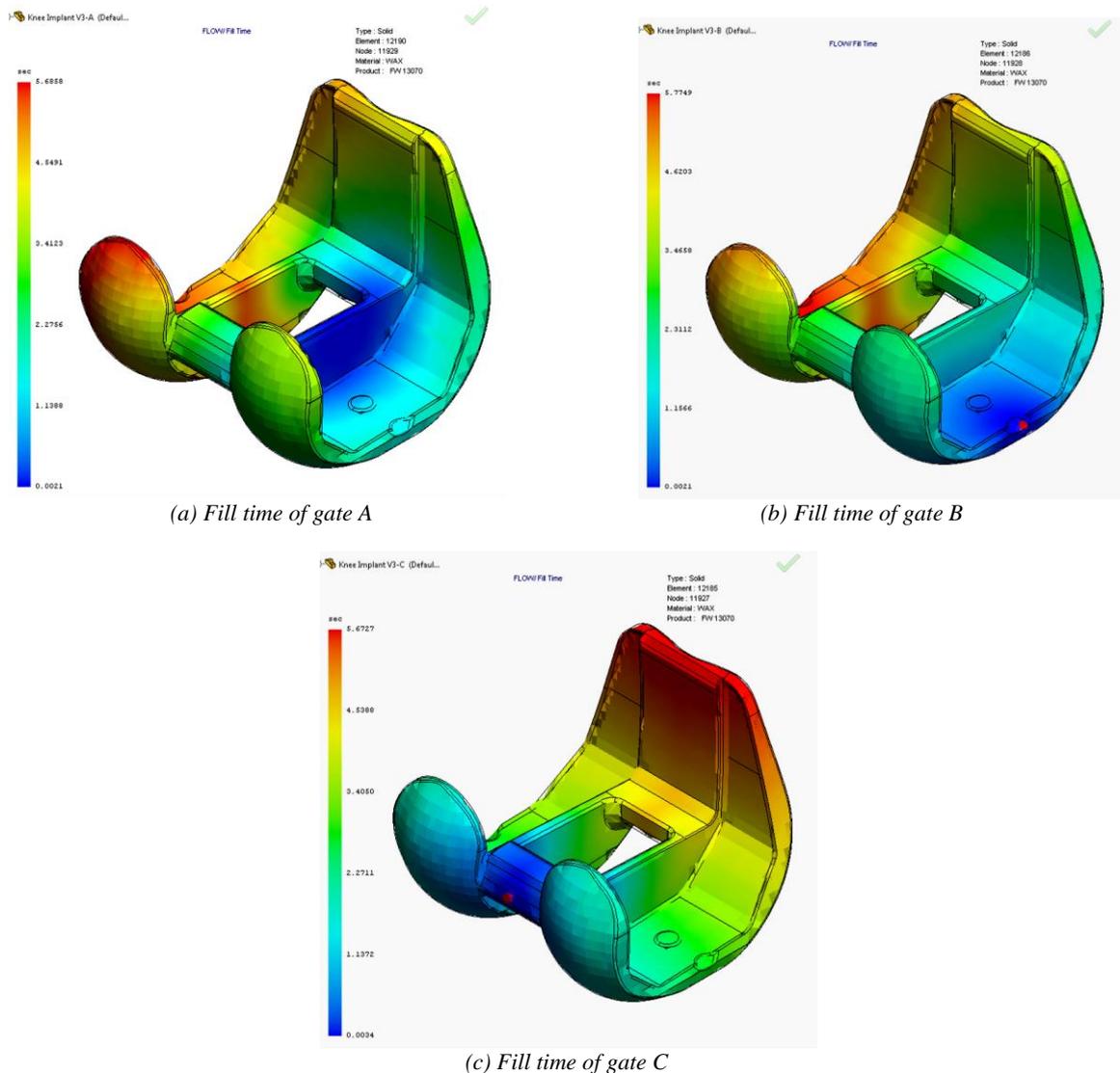

(a) Fill time of gate A

(b) Fill time of gate B

(c) Fill time of gate C

Fig 17. Fill times of different gate location.

Table 7 shows the results of the simulation performed in SolidWorks Plastics with 12 different variations. Two different values of injection rate, 10 cm³/s and 15 cm³/s, were assigned in the simulation, while the melting temperature and the mould temperature had four different values each, from the minimum to the maximum, in the rage recommended by the manufacturer. The melting temperatures of the wax were 67°C, 69°C, 71°C and 73°C and the mould temperatures were 20°C, 25°C, 30°C and 35°C.

The Flow/Pack switch point becomes important if the packing stage is taken into account and the process control must switch to a pressure control before the cavity is fully filled. Flow/Pack switch points with the values ranging from 97% to 100 % were analyzed. Pressure holding time and cooling time were switched to Auto mode.

Table 7 indicates that the shortest fill time was for variation 12 and it equalled 3.7774 s. In this variation higher injection rate of 15 cm³/s was used while the wax and the mould temperature parameters were at the maximum (73°C and 35°C). Flow/Pack switch point was set at 100%.

When comparing the couples of variations 5 and 6 and 11 and 12, it could be noticed that if the mould temperature is lowered, the fill time rises.

The data about different parameters of the process in different phases of wax injection were obtained as the result of the simulation:

- Flow results: fill time, pressure, temperature, flow front central temperature, shear rate and shear stress, volume shrinkage, sink marks, velocity, weld lines, air traps;

- Pack results: pressure, temperature, shear stress and shear rate, volume shrinkage, residual stress;

- Warp results: Sink-Mark profile, stress, displacement.

Fig. 18 shows the positions in which air traps and weld lines occur during injection. With certain design changes we can localize the air traps in the zones where they can be later extruded from the cavity by mould design without any consequences. The weld lines are defects occurring when two fronts of melted and cooled wax meet. These defects may be avoided if certain design changes and gate location changes are made.
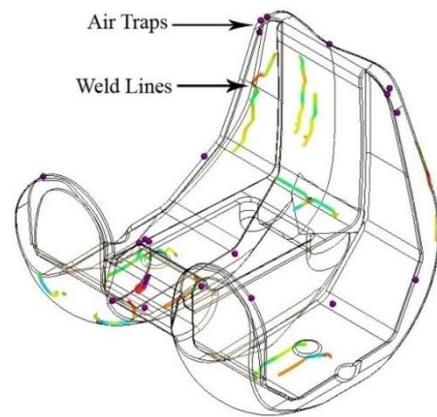

Fig. 18. Air traps and Weld lines.

Simulation results also show that progression of flow front (64.11°C - 69°C) is closely related with the injection temperature and pressure (Fig. 19). Flow front central temperature is the temperature distribution at each region when the flow reaches.
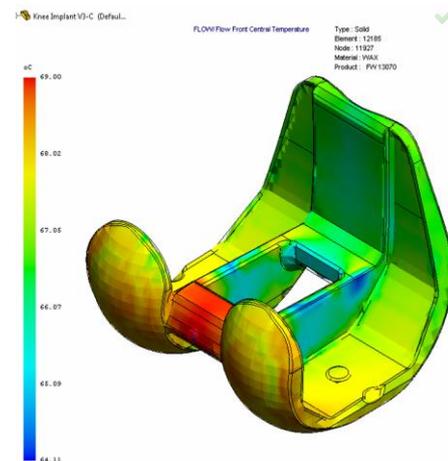

Fig. 19. Flow Front central temperature

Table 7. Numerical simulation results.

S/N	Variable settings							
	Injection rate [cm³/s]	Melting temperature of wax [°C]	Mould temperature [°C]	Flow/Pack switch point [%]	Pressure holding time [s]	Cooling time [s]	Fill time [s]	Filling percentage [%]
#1	10	67	20	97	9.17	18.78	5.7612	100
#2	10	67	35	97	9.17	23.28	5.8154	100
#3	10	69	25	98	9.17	20.07	5.7477	100
#4	10	71	30	99	9.17	21.88	5.6897	100
#5	10	73	20	97	9.17	19.71	5.8078	100
#6	10	73	35	100	9.17	24.63	5.6584	100
#7	15	67	20	97	9.17	18.78	3.8634	100
#8	15	67	35	97	9.17	23.27	3.8686	100
#9	15	69	25	98	9.17	20.07	3.8242	100
#10	15	71	30	99	9.17	21.92	3.7869	100
#11	15	73	20	97	9.17	19.70	3.8881	100
#12	15	73	35	100	9.17	24.68	3.7774	100

The final product is shown in Fig. 20 (a), with a three different knee implant AM models: SLS model - Fig. 20 (b), 3DP model - Fig. 20 (c) and PJP model - Fig. 20 (d).

Fig. 20. Finished knee implant pattern models:(a) wax pattern, (b) SLS model, (c) 3DP model and (d) PJP model.

Comparison of AM pattern material properties may be seen in Table 8.

Table 8. Properties of finished implant prototypes.

Technology	SLS	3DP	PJP
Material	PA 2200	zp151	Vero Black
Tensile strength [MPa]	45	26	50.7
Modulus of elasticity [MPa]	1700	10680	2192
Elongation [%] at yield	15	0.2	17.7 (at break)
Impact strength (notched Izod test) [J/m]	32.8	n/a	23.9
Hardness Shore Scale D	75	87	83
Layer thickness [mm]	0.1	0.0889	0.028
Accuracy [%]	0.5-1	1-4	0.2
Surface roughness	rough and porous	rough and textured	very high quality

Materials used in this research were the base materials used for functional prototypes. In this phase of the research, materials exclusively recommended by the manufacturer as the materials used in investment casting, were not available. The manufacturers of the analyzed AM systems offer materials which can replace standard wax models, such as:

− SLS material PrimeCast 101;
− 3DP material zp14;
− PJP material PolyJet FullCure 700.

The comparison of print time for the three processes is shown in Table 9.

Table 9. Print time need for multi model manufacturing.

Number of models	SLS Formiga P100 [h:min]	3DP Spectrum Z510 [h:min]	PJP Objet 30 [h:min]
1	1:58	3:09	16:37
2	3:27	3:19	18:12
4	6:35	3:54	26:55
6	10:34	4:18	29:07

The SLS process is the fastest if one model printing is considered mainly because of the printing layer thickness (SLS − 0.1 mm, 3DP − 0.0889 mm and PJP − 0.028 mm). On the other hand, 3DP process is the fastest for the multi model manufacturing if arranged in one row on the platform due to the print head width.

Table 10 shows the material consumption for a model of implant.

Table 10. Material consumption for one model.

Parameter	SLS	3DP	PJP
Total volume [cm^3]	49.26	49.26	49.26
Total surface area [cm^2]	197.79	197.79	197.79
Surface to volume ratio	10.20	10.20	10.20
Model material	PA 2200	zp151	Vero Black
Consumption [l], [g]	0.175 [l]	0.133 [l]	117 [g]
Support material	-	ZB60	FullCure 705
Consumption [l], [g]	-	0.038 [l]	94 [g]

6. Conclusions

The synergy produced by uniting CAD/CAE, Reverse Engineering using optical scanner, Additive Manufacturing technology and IC process, is an outstanding contribution of engineering in medical sciences.

The research confirmed that the optimal gate location may be determined by numerical simulation resulting in shortening the fill time and increasing the percentage of cavity filling. The simulation results also indicate the

relationship between the status of flow front and wax filling time, pressure and temperature. With the simulation of SolidWorks Plastics, the results could be predicated, and the quality of product could be improved with the low cost. Conclusions from simulation results have proved to be extremely useful being used in experimental research on investment casting of complex medical implants.

Instead of making tools, AM patterns could be directly fabricated from a design engineer's CAD solid model within a matter of hours and provide a casting in a matter of days. Each of the type of AM processes described in this research had its own advantages and limitations, and so it depends upon the end-user to select the appropriate AM technique in conjunction with the IC process to manufacture a part in an efficient manner.

The SLS, 3DP and PJP technologies can be used to create complex objects, like knee implants and to use these objects for investment casting process as non wax pattern or for AM-fabricated moulds for wax injection (indirect tooling). Also, by using the SLS, 3DP and PJP patterns it is possible to make a silicon mould and with it cast the wax patterns in the vacuum chamber. Investment casting technology is applied hereafter.

The paper ends with a hope that in the future, application of numerical simulation and AM technology in investment casting solutions will emerge with the capability to provide dimensionally more accurate and better surface size, shape and material with more speed and low costs.

Acknowledgements

References

[1] W. Bonilla, S. H. Masood, P. Iovenitti, Bulletin of Industrial Research Institute of Swineburne, Melbourne, Australia, **18**, 348 (2001).

[2] J.C. Gebelin, M.R. Jolly, Journal of Material Processing Technology, **135**, 291 (2003).

[3] A.S. Sabau, S. Viswanathan, Material Science and Engineering, **A362**, 125 (2003).

[4] B. He, D. Wang, F. Li, B. Sun, Advanced Materials Research, **834-836**, 1575 (2014).

[5] S. A. Radu, D. F. Fratila, Proceedings of the Romanian Academy, Series A, **13**(4), 343 (2012).

[6] M. Chhabra, R. Singh, Rapid Prototyping Journal, **17**(5), 328 (2011).

[7] I. Gibson, Advanced Manufacturing Technology for Medical Applications, Reverse Engineering, Software Conversion and Rapid Prototyping, John Wiley & Sons Ltd. (2005).

[8] M. Horacek, O. Charvat, T. Pavelka, J. Sedlak, M. Madaj, J. Nejedly, J. Dvoracek, China Foundry, **8**(1), 107 (2011).

[9] P.K. Maji, P.S. Banerjee, A. Sinha, Int J Adv Manuf Technol **36**, 510 (2008).

[10] A.M. Ramos, J. A. Simoes, Rapid Prototyping Journal, **15**(3), 211 (2009).

[11] A. Rajic, E. Desnica, S. Stojadinovic, D. Nedelcu, Facta Universitatis, Series: Mechanical Engineering, **11**(1), 45 (2013).

[12] Y. Jun, International Journal of Advanced Manufacturing Technologies, **52**(9-12), 841 (2011).

[13] M. Horacek, Latest trends in investment casting technology, Innovative Foundry Materials and Technologies, Varazdin, University of Zagreb, Croatia, 7 (2005)

[14] EOS GmbH Electro Optical Systems. Formiga P100 prototyping machine datasheet, polyamide PA 2200 properties, from http://www.eos.info/systems_solutions/plastic/systems_eq uipment/formiga_p_110 and http://eos.materialdatacenter.com/eo/standard/main/ds, accessed on 2014-06-17.

[15] M. Toth-Tascau, D. I. Stoia, Optoelectron. Adv. Mater. – Rapid Comm., **5**(12), 1356 (2012).

[16] I. Gibson, D.W. Rosen, B. Stucker, Additive Manufacturing Technologies: Rapid Prototyping to Direct Digital Manufacturing, Springer, (2010).

[17] 3D Systems. Z Corp. Spectrum Z510 prototyping machine, datasheet, powder zp151 properties from http://www.3dsystems.com/press-releases/z-corps-spectrum-z510-full-col and https://3dscentral.3dsystems.com/attachments/2238_95034 %20zp151%20User%20Guide.pdf, accessed 2014-06-17.

[18] C.M. Cheah, C.K. Chua, C.W. Lee, C. Feng, K. Totong, International Journal of Advanced Manufacturing Technology, **25**(3-4), 308 (2005).

[19] M. Stanek, D. Manas, M. Manas, J. Navratil, K. Kyas, V. Senkerik, A. Skrobak, International Journal of Mathematics and Computers in Simulation, **6**(6), 550 (2012).

[20] Stratasys Ltd. Objet 30 prototyping machine datasheet, VeroBlack FullCure 870 properties from http://www.stratasys.com/3d-printers/technologies/polyjet-technology and http://www.stratasys.com/~/media/Main/Secure/Mater ial%20Specs%20MS/PolyJet-Material-Specs/PolyJet_Materials_Data_Sheet.pdf accessed 2014-06-17, accessed 2014-06-17.

---

* Corresponding author: aleksandarrajic@yahoo.com